

RESEARCH

Open Access



Chemical screen in zebrafish lateral line identified compounds that ameliorate neomycin-induced ototoxicity by inhibiting ferroptosis pathway

Yipu Fan^{1,2,3†}, Yihan Zhang^{4†}, Dajiang Qin^{1,4,5} and Xiaodong Shu^{2,6*} 

Abstract

Background Ototoxicity is a major side effect of many broadly used aminoglycoside antibiotics (AGs) and no FDA-approved otoprotective drug is available currently. The zebrafish has recently become a valuable model to investigate AG-induced hair cell toxicity and an expanding list of otoprotective compounds that block the uptake of AGs have been identified from zebrafish-based screening; however, it remains to be established whether inhibiting intracellular cell death pathway(s) constitutes an effective strategy to protect against AG-induced ototoxicity.

Results We used the zebrafish model as well as in vitro cell-based assays to investigate AG-induced cell death and found that ferroptosis is the dominant type of cell death induced by neomycin. Neomycin stimulates lipid reactive oxygen species (ROS) accumulation through mitochondrial pathway and blocking mitochondrial ferroptosis pathway effectively protects neomycin-induced cell death. We screened an alkaloid natural compound library and identified seven small compounds that protect neomycin-induced ototoxicity by targeting ferroptosis pathway: six of them are radical-trapping agents (RTAs) while the other one (ellipticine) regulates intracellular iron homeostasis, which is essential for the generation of lipid ROS to stimulate ferroptosis.

Conclusions Our study demonstrates that blocking intracellular ferroptosis pathway is an alternative strategy to ameliorate neomycin-induced ototoxicity and provides multiple hit compounds for further otoprotective drug development.

Keywords Aminoglycoside, Neomycin, Ototoxicity, Ferroptosis, Zebrafish

[†]Yipu Fan and Yihan Zhang contributed equally to this work.

*Correspondence:

Xiaodong Shu
shu_xiaodong@gibh.ac.cn

¹Centre for Regenerative Medicine and Health, Hong Kong Institute of Science & Innovation, Chinese Academy of Sciences, Hong Kong SAR, China

²Guangdong Provincial Key Laboratory of Stem Cell and Regenerative Medicine, Guangzhou Institutes of Biomedicine and Health, Chinese Academy of Sciences, Guangzhou 510530, China

³University of Chinese Academy of Sciences, Beijing 100049, China

⁴Bioland Laboratory, Guangzhou Regenerative Medicine and Health Guangdong Laboratory, Guangzhou 510005, China

⁵Key Laboratory of Biological Targeting Diagnosis, Therapy and Rehabilitation of Guangdong Higher Education Institutes, The Fifth Affiliated Hospital, Guangzhou Medical University, Guangzhou 510700, China

⁶School of Biological and Chemical Engineering, Zhejiang University of Science and Technology, Hangzhou 310023, China



© The Author(s) 2024. **Open Access** This article is licensed under a Creative Commons Attribution 4.0 International License, which permits use, sharing, adaptation, distribution and reproduction in any medium or format, as long as you give appropriate credit to the original author(s) and the source, provide a link to the Creative Commons licence, and indicate if changes were made. The images or other third party material in this article are included in the article's Creative Commons licence, unless indicated otherwise in a credit line to the material. If material is not included in the article's Creative Commons licence and your intended use is not permitted by statutory regulation or exceeds the permitted use, you will need to obtain permission directly from the copyright holder. To view a copy of this licence, visit <http://creativecommons.org/licenses/by/4.0/>. The Creative Commons Public Domain Dedication waiver (<http://creativecommons.org/publicdomain/zero/1.0/>) applies to the data made available in this article, unless otherwise stated in a credit line to the data.

Introduction

Aminoglycoside antibiotics (AGs, such as neomycin, gentamicin, tobramycin, amikacin, kanamycin, streptomycin, etc.) are broad-spectrum antibiotics that function by irreversibly binding to the 16 S rRNA in the 30 S subunit of bacterial ribosome to disrupt bacterial protein synthesis. Ototoxicity and nephrotoxicity are the two major AG-induced side effects in patients. AGs are transported into hair cells via channels such as mechanotransducer or transient receptor potential where they bind to mitochondrial rRNA and this ribotoxicity is proposed to be critical for AG-induced ototoxicity [1–4]. Mechanistically, AGs induce mitochondrial dysfunction and generate toxic level of intracellular ROS which then leads to hair cell death via multiple intracellular death pathways [4–6]. Based on these discoveries, many drugs or pre-clinical compounds that can either block AG uptake or scavenge AG-induced ROS have been reported to be otoprotective in cell-based assays or various animal models, however, none of them has been FDA-approved as otoprotective drug so far.

Ferroptosis is a recently discovered form of regulated cell death that is involved in an expanding list of diseased conditions [7–9]. A hallmark of ferroptosis is the accumulation of detrimental level of lipid peroxides which are generated via either Fenton reaction or enzymatic pathways in an iron-dependent manner [10]. Meanwhile, cells have evolved multiple pathways which include the GPX4/GSH pathway, the FSP1/CoQ pathway, the GCH1/BH4 pathway and the mitochondrial DHODH/CoQ pathway to remove excessive lipid peroxides and suppress ferroptosis [8, 11]. Small chemical compounds that inhibit these defensive pathways are able to induce ferroptosis while iron chelators or RTAs inhibit ferroptosis [12]. Several previous studies indicate that lipid ROS and ferroptosis might be involved in AG-induced hair cell damages, for example, the iron chelator deferoxamine partially protects gentamicin-induced hair cell death in cultured guinea pig cochlear neurosensory epithelium [13] and attenuates gentamicin- or neomycin-induced hearing loss in guinea pig in vivo [14, 15]. Sodium selenite which is a GPX4 activator protects against neomycin-induced hair cell damage in zebrafish [16]. The broadly used ferroptosis inhibitor Liproxstatin-1, which is a RTA, reduces neomycin-induced ROS production and cell death in cultured HEI-OC1 cells and cochlear explants [17]. However, direct evidence for a pathogenic role of ferroptosis during AG-induced ototoxicity remains to be established.

AG-induced ototoxicity is traditionally investigated in animal models such as mice, rats, guinea pigs, etc [3]. Recently, zebrafish has become an attractive model for ototoxicity researches [18]. AGs such as neomycin and gentamicin have been established to induce hair cell death in zebrafish inner ear and lateral line [19, 20]

and mitochondrial defect has been identified as an early event in neomycin-induced hair cell death in zebrafish [21]. Further study reveals that mitochondrial calcium-driven ROS generation is essential for neomycin-induced hair cell death as mitochondrial-targeted ROS scavenger effectively protects against neomycin ototoxicity [22]. Additional compounds such as trimetazidine, edaravone, Necro-5, ecabet sodium, quercetin are reported to have otoprotective activities against neomycin-induced hair cell death in zebrafish, possibly functioning as RTAs as well [23–27]. In addition to ROS scavenging, blocking the uptake of AGs is another effective way to protect hair cells from AG-induced ototoxicity. For example, berbamine and its derivative compounds, isotetrandrine, d-tubocuraine and ORC-13,661 are reported to protect zebrafish lateral line hair cells from neomycin- or gentamicin-induced ototoxicity by this mechanism [28–31]. Zebrafish is also used as an in vivo screening model to identify additional otoprotective compounds. Screens of several targeted or commercial compound libraries against AG-induced hair cell damage in zebrafish lateral line have been performed and compounds with either previous known or unknown otoprotective activities have been identified [28, 32–37]. Further investigation of these hit compounds will not only shed light on the mechanisms of AG-induced ototoxicity but also provide lead compounds for further otoprotective drug development.

In this study, we report that neomycin induces ferroptosis in zebrafish lateral line hair cells through mitochondrial ROS pathway. Blocking ferroptosis by reducing mitochondrial ROS or lipid ROS prevents AG-induced hair cell damage. We performed a small compound screen and identified additional otoprotective compounds that inhibit ferroptosis and act as either RTAs or regulator of iron homeostasis.

Results

Analysis for the relative contributions of apoptosis, necroptosis and ferroptosis pathways in zebrafish hair cell damages induced by various ototoxins

To assess potential contributions of various cell death pathways in AG-induced hair cell toxicity, we first performed otoprotection assay using pathway specific inhibitors. Zebrafish larvae at 5 day post fertilization (*dpf*) were pre-incubated with either a ferroptosis inhibitor [38] (Liproxstatin-1, 10 μ M), apoptosis inhibitor [39] (Z-VAD-FMK, 50 μ M), necroptosis inhibitor [40] (Necrostatin-1, 50 μ M) or the general antioxidant N-acetylcysteine which at high concentration ameliorates either necroptosis or ferroptosis (NAC, 5 mM) for 2 h then treated with 125 μ M neomycin for 2 h. Treated larvae were stained with 2-[4-(Dimethylamino)styryl]-1-ethylpyridinium iodide (DASPEI, a mitochondrial dye that labels vital hair cells) and 4',6-diamidino-2-phenylindole (DAPI, which labels

hair cell nuclei), imaged under a confocal microscope and the number of vital hair cells per neuromast was counted (at least 10 larvae were assayed in each treatment). A typical result of otoprotection against neomycin-induced hair cell damage is present in Fig. 1A and it reveals that Liproxstatin-1 effectively protects neomycin-induced ototoxicity, NAC has mild protective activity while Z-VAD-FMK or Necrostatin-1 has no detectable protective activity at all. These observations indicate that ferroptosis is the dominant cell death induced by neomycin.

We then analyzed additional AG-induced hair cell damages (streptomycin, gentamicin, and amikacin) using similar protocols and found that streptomycin-induced hair cell death can be protected by Liproxstatin-1 but not Z-VAD-FMK or Necrostatin-1 (Fig. 1B), which is very similar to neomycin-induced hair cell damage. On the other hand, gentamicin- or amikacin-induced hair cell damages can be partially rescued by Liproxstatin-1,

Z-VAD-FMK, Necrostatin-1, or NAC (Fig. 1C, D), indicating that ferroptosis, apoptosis and necroptosis all partially contribute to hair cell damages induced by these AGs. We also analyzed cisplatin and CuSO₄ (two well-established ototoxic reagents in zebrafish) [20, 41] induced hair cell damage and found that cisplatin-induced ototoxicity can be protected by apoptosis and necroptosis inhibitor but not ferroptosis inhibitor (Fig. 1E) while CuSO₄-induced hair cell death can be blocked by necroptosis inhibitor or NAC but not ferroptosis or apoptosis inhibitor (Fig. 1F). Together, these data indicate that various intracellular cell death pathways are activated by different ototoxic reagents and ferroptosis is the dominant cell death induced by neomycin or streptomycin, it also contributes to gentamicin- or amikacin-induced hair cell death but it is dispensable for cisplatin- or CuSO₄-induced hair cell death.

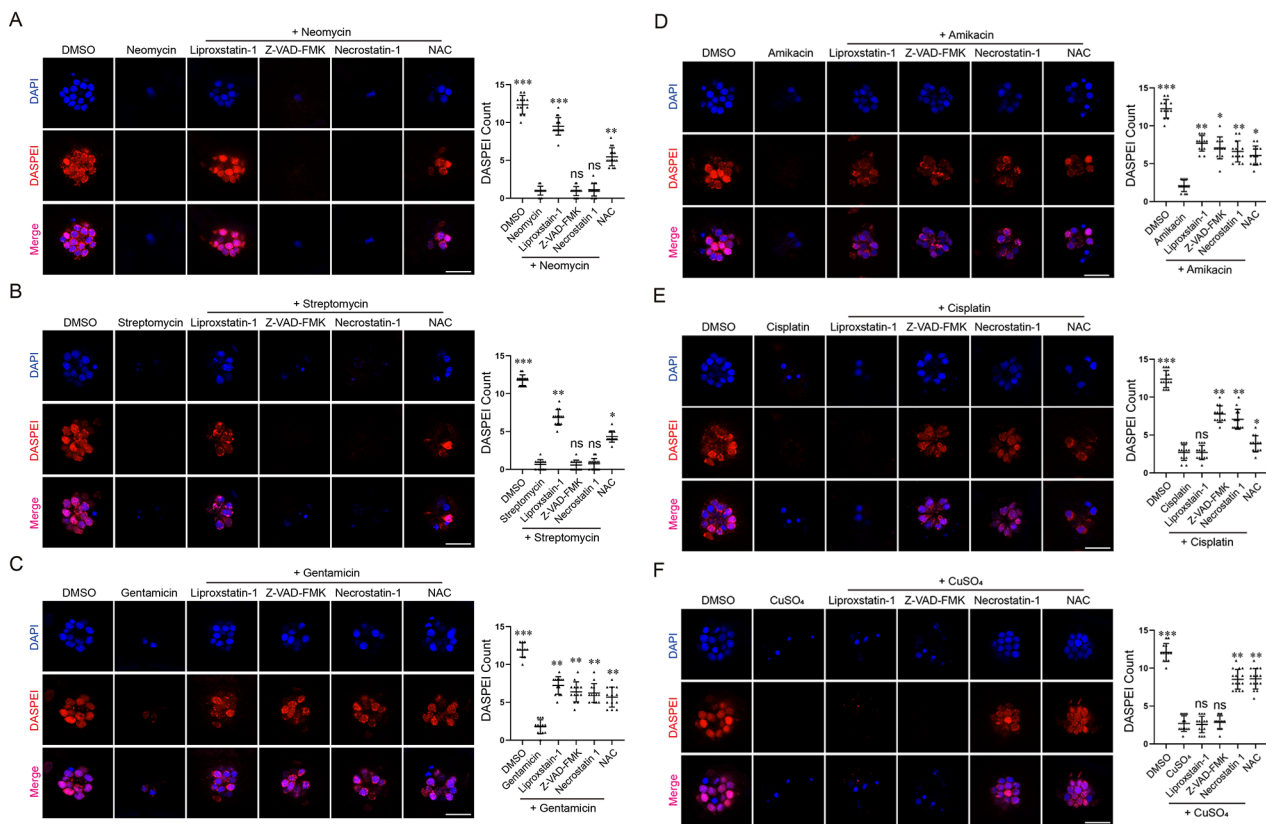


Fig. 1 Otoprotection against various ototoxin-induced lateral line neuromast damage by inhibitors of different cell death pathways. Typical confocal images and quantitative results of otoprotection assay. **(A)** The ferroptosis inhibitor Liproxstatin-1 effectively blocks neomycin-induced hair cell death. The non-specific antioxidant NAC shows partial protective activity while apoptosis inhibitor (Z-VAD-FMK) and necroptosis inhibitor (Necrostatin-1) are not effective in this assay. **(B)** Liproxstatin-1 and NAC also partially protect against streptomycin-induced hair cell death. **(C, D)** Gentamicin- or amikacin-induced hair cell death can be partially protected by Liproxstatin-1, Z-VAD-FMK, Necrostatin-1, or NAC. **(E)** Cisplatin-induced hair cell damage is ameliorated by Z-VAD-FMK, Necrostatin-1, NAC but not Liproxstatin-1. **(F)** Copper-induced hair cell death is protected by Necrostatin-1 or NAC, but not Liproxstatin-1 or Z-VAD-FMK. Three biological repeats were performed for each assay and at least ten larvae were analyzed for each treatment. Data represent mean \pm s.d. and *p*-value is determined by ordinary one-way ANOVA with Dunnett’s multiple comparisons test. ns, no significance; *, *p* < 0.05; **, *p* < 0.01; ***, *p* < 0.001. Scale bar in **A-F**: 20 μ m

Neomycin induces lipid ROS accumulation in hair cells

Accumulation of lipid ROS is a hallmark of ferroptosis. While it can be readily detected in various cell cultures during ferroptosis, *in vivo* detection of the accumulation of lipid ROS remains challenging. We took advantage of the imaging capacity of zebrafish larvae and investigated whether neomycin induces ROS (total ROS and lipid ROS) accumulation in hair cells *in vivo*. For detection of total ROS, larvae were first incubated with the dichlorodihydrofluorescein diacetate (DCFH-DA) probe (DCF, 10 min), stimulated with neomycin (125 μ M, 15 min) then imaged under a confocal microscope. We found that neomycin treatment clearly induces the accumulation of total intracellular ROS in hair cells which can be scavenged by NAC or Lipoxstatin-1 but not Z-VAD-FMK or Necrostatin-1 (Fig. 2A). We then detected lipid ROS

by Liperfluo staining and found that neomycin induces a transient accumulation of lipid ROS which is blocked by Lipoxstatin-1 or NAC (Fig. 2B). These data further support that neomycin induces ferroptosis in hair cells.

Neomycin and Fe³⁺ synergistically sensitize cells to ferroptosis through mitochondrial ROS pathway

To investigate the mechanism of neomycin-stimulated ferroptosis, we used the HT1080 cell model which is routinely used in ferroptosis-related studies. We found that neomycin alone (up to 5 mM) does not induce HT1080 cell death (Fig. S1A) and neomycin (200 to 800 μ M) does not stimulate ferroptosis sensitivity to RSL3 (Fig. S1B), indicating neomycin alone is not sufficient to stimulate ferroptosis in this cell line. We noticed that a previous biochemical study reported that gentamicin promotes

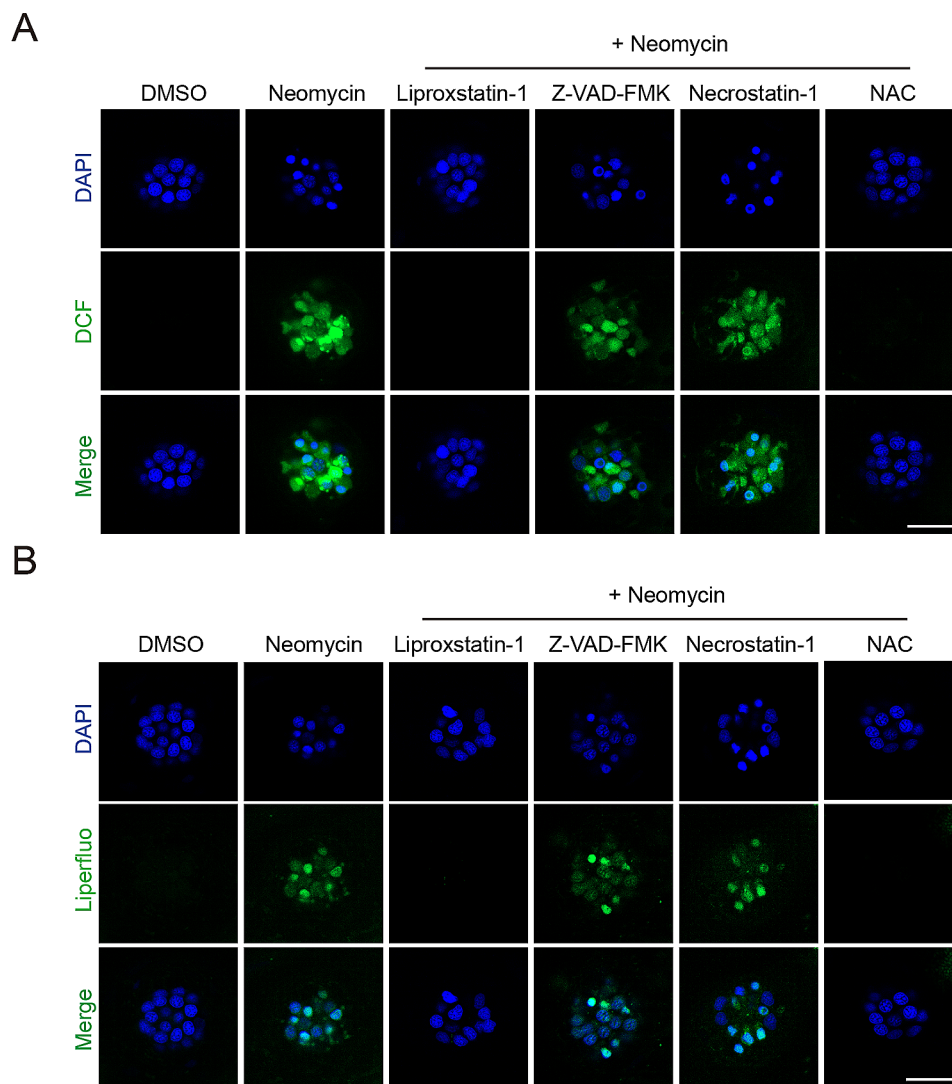


Fig. 2 ROS staining in hair cells. Representative confocal images of DCF staining (**A**, for total ROS) or Liperfluo staining (**B**, for lipid ROS) are shown. Neomycin induces the accumulation of total ROS as well as lipid ROS, which can be blocked by Lipoxstatin-1 and NAC, but not Z-VAD-FMK and Necrostatin-1. Assays were repeated twice. Scale bar in **A-B**: 20 μ m

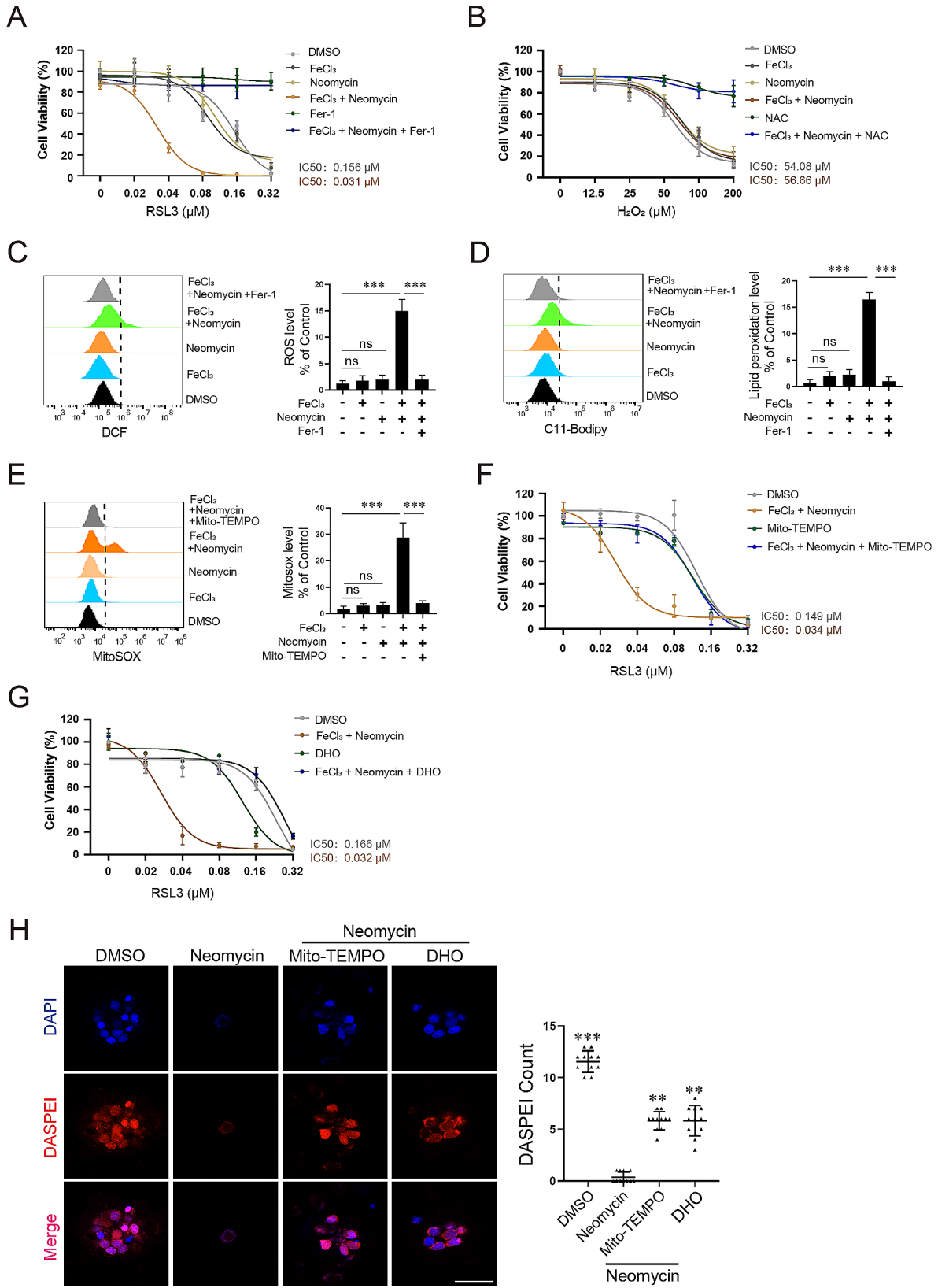


Fig. 3 (See legend on next page.)

(See figure on previous page.)

Fig. 3 Neomycin and Fe^{3+} synergistically sensitize HT1080 cells to ferroptosis inducer RSL3. **(A)** Cell viability assay. Neomycin (500 μM) or Fe^{3+} iron (5 μM) treatment alone has minor effect on ferroptosis sensitivity to RSL3, however, a combination of them dramatically sensitizes HT1080 cells to RSL3-induced ferroptosis. Data represent mean \pm s.d. from three independent experiments. **(B)** Neomycin, iron or their combination does not sensitize HT1080 cells to H_2O_2 -induced cell death. Assays were performed and data were analyzed as described in **(A)**. **(C, D)** FACS analysis of total ROS **(C, DCF staining)** or lipid ROS **(D, C11-Bodipy staining)** in the treated cells. Neomycin and iron synergistically induce total ROS as well as lipid ROS (in the absence of RSL3), which can be blocked by the ferroptosis inhibitor Fer-1 which is an RTA. Data represent mean \pm s.d. from three biological repeats and p -value is determined by ordinary one-way ANOVA with Tukey's multiple comparisons test. ns, no significance; ***, $p < 0.001$. **(E)** Neomycin and iron synergistically induce mitochondrial ROS (MitoSOX staining) which is blocked by the mitochondria-targeted antioxidant Mito-TEMPO. Data represent mean \pm s.d. from three biological repeats and p -value is determined by ordinary one-way ANOVA with Tukey's multiple comparisons test. ns, no significance; ***, $p < 0.001$. **(F)** Mito-TEMPO (20 μM) reverses ferroptosis sensitivity to RSL3 in HT1080 cells stimulated by the combination of neomycin and iron. Data represent mean \pm s.d. from three independent experiments. **(G)** The neomycin/iron stimulated ferroptosis sensitivity to RSL3 is abolished by DHO treatment (200 μM), which activates the mitochondrial DHODH/CoQ pathway to defense against ferroptosis. Data represent mean \pm s.d. from three biological repeats. **(H)** Mito-TEMPO (20 μM) or DHO (200 μM) partially alleviates neomycin-induced hair cell death. Data represent mean \pm s.d. and p -value is determined by ordinary one-way ANOVA with Dunnett's multiple comparisons test. **, $p < 0.01$; ***, $p < 0.001$. Scale bar: 20 μm

ferric or ferrous ion mediated lipid peroxidation in vitro [42], so we hypothesized that neomycin might synergize with iron to modulate ferroptosis sensitivity in HT1080 cells. We found ferric iron alone (up to 80 μM) does not induce HT1080 cell death (Fig. S1C) and ferric iron at 5–20 μM range has minor effect on ferroptosis sensitivity to RSL3 (Fig. S1D). However, a combination of iron (5 μM) and neomycin (500 μM) dramatically sensitizes HT1080 cells to RSL3-induced cell death (IC_{50} decreased from 156 to 31 nM) (Fig. 3A). Furthermore, this cell death can be fully rescued by ferroptosis inhibitor ferrostatin-1 (Fer-1) (Fig. 3A), indicating it is ferroptosis. Erastin and sorafenib are two other commonly used ferroptosis inducers and we found that the combination of neomycin with iron also sensitizes HT1080 cells to cell death induced by these agents (Fig. S2). We then determined whether neomycin/iron affects cell death induced by hydrogen peroxide (ROS-dependent necroptotic cell death) and found that it does not promote hydrogen peroxide induced necroptosis (Fig. 3B), indicating that iron and neomycin favor the generation of lipid ROS. We next measured the levels of total cellular ROS as well as lipid ROS in control, iron, neomycin, and iron plus neomycin treated cells (all in the absence of RSL3) and found that the combination of iron and neomycin synergistically induces the generation of total and lipid ROS (Fig. 3C, D), which is likely to be responsible for the elevated ferroptosis sensitivity in those treated cells.

AGs are well-established to induce mitochondrial dysfunction and stimulate mitochondrial ROS generation in hair cells which is responsible for AG-induced ototoxicity. So, we determined whether neomycin and iron stimulate ferroptosis through mitochondrial ROS pathways. We found that neomycin (500 μM) or iron (5 μM) alone is not sufficient to stimulate mitochondrial ROS in HT1080 cells, however, a combination of neomycin with iron dramatically stimulates the accumulation of mitochondrial ROS, which can be removed by the administration of mitochondria-targeted ROS scavenger Mito-TEMPO (Fig. 3E). Furthermore, Mito-TEMPO treatment also abolishes neomycin/iron combination

induced ferroptosis sensitivity (Fig. 3F). We noticed that Mito-TEMPO does not modulate RSL3 sensitivity in the absence of neomycin/iron (Fig. 3F), indicating that it does not affect RSL3 signaling. To further investigate the involvement of mitochondrial ROS pathway in neomycin/iron stimulated ferroptosis sensitivity, we tested whether dihydroorotate (DHO, 200 μM) which protects ferroptosis through the mitochondrial DHODH/CoQ pathway [43] can block neomycin/iron stimulated ferroptosis sensitivity and found that DHO treatment effectively abolishes neomycin/iron stimulated ferroptosis sensitivity (Fig. 3G). We then investigated whether a similar mechanism underlies neomycin-induced hair cell death in vivo. In line with the aforementioned results, we found that both Mito-TEMPO (20 μM) and DHO (200 μM) are able to ameliorate neomycin-induced hair cell death in larvae (Fig. 3H). Together, these data indicate that ferroptosis induced by mitochondrial ROS pathway is responsible for neomycin ototoxicity.

Chemical screen in zebrafish identifies multiple otoprotective compounds that ameliorate neomycin-induced hair cell death by blocking ferroptosis pathway

Previous studies have identified many otoprotective compounds against AG-induced hair cell damage and most of them function to block the uptake of AGs [28, 33–35]. Our discovery that neomycin-induced hair cell death is dominated by ferroptosis (unlike gentamicin or cisplatin) indicates that an otoprotection screening under our assay condition might identify additional otoprotective compounds that function to block the ferroptosis pathway. To this end, we screened an alkaloid natural compound library (Table S1) for compounds that can ameliorate neomycin-induced hair cell damage in zebrafish larvae. Briefly, zebrafish larvae at 5 dpf were first treated with a testing compound (10 μM) then incubated with neomycin (125 μM) for 2 h. Treated embryos were stained with DASPEI then visually examined under a fluorescence microscope. A typical visual screening result is presented in Fig. S3. Positive hits were retested, and the treated larvae were imaged under a confocal microscope. We totally

identified nine compounds with variable otoprotective activities from the screen (Fig. 4A, B). To dissect their otoprotective mechanisms, we first tested whether these compounds block the uptake of AG by GTTF4 loading assay. We found that dronedarone and quinine strongly inhibit the uptake of GTTF4 while other hit compounds show either weak (berbamine and catharanthine) or negligible (cepharanthine, ellipticine, fangchinoline, liensinine and isoliensinine) channel blocker activity (Fig. 5), indicating these compounds have additional otoprotective mechanism(s).

We noticed that five of them (berbamine, cepharanthine, fangchinoline, liensinine and isoliensinine) belong to the bisbenzylisoquinoline (BBIQ) compounds that we recently identified as RTAs and ferroptosis inhibitors [44]. Consistent with our previous studies, we found these BBIQ compounds effectively block RSL3-induced ferroptosis in HT1080 cells (Fig. 6A). We then tested whether other hit compounds also have ferroptosis inhibiting activities in HT1080 cells and found that catharanthine and ellipticine can inhibit RSL3-induced ferroptosis while dronedarone and quinine do not have ferroptosis inhibiting activity (Fig. 6A). We next measured their ability to block RSL3-induced lipid ROS accumulation in HT1080 cells (ellipticine was excluded from this assay due to strong autofluorescence) and found that catharanthine as well as the five BBIQ compounds all reduce lipid ROS accumulation (Fig. 6B). We then assayed whether these six compounds have similar ROS scavenging activities in vivo and found that all of them can block neomycin-induced lipid ROS accumulation in hair cells (Fig. 6C). Together, our screen identified nine otoprotective compounds that either block neomycin uptake (2 out of 9) or neomycin-induced ferroptosis (7 out of 9).

Ellipticine inhibits ferroptosis through down-regulation of TFRC and cell iron content

Ellipticine is a natural compound that inhibits DNA topoisomerase II and stimulates cell death in a variety of tumor cell lines, which appears contradictory to the anti-cell death activity we report here. So, we further investigated ellipticine in cell viability assay. We found that ellipticine dose-dependently induces HT1080 cell death at micromolar level ($IC_{50}=4.93 \mu\text{M}$) (Fig. 7A) while it is able to inhibit RSL3-induced ferroptosis at sub-micromolar level (peaked at $0.5 \mu\text{M}$, Fig. 7B). It also blocks neomycin/ Fe^{3+} stimulated ferroptosis sensitivity to RSL3 (Fig. 7C). The anti-cell death activity of ellipticine is ferroptosis-specific as it does not block hydrogen peroxide induced necroptosis or staurosporine-induced apoptosis in the same cell line (Fig. 7D). We evaluated ROS scavenging capacity of ellipticine by in vitro DPPH assay and found it has no ROS scavenging activity (Fig. 7E),

indicating it inhibits ferroptosis by mechanism(s) other than RTA.

To investigate the anti-ferroptotic mechanism of ellipticine, we first analyzed whether ellipticine affects protein levels of key ferroptosis regulators by western blot. We found that the protein levels of GPX4, SLC7A11, HO-1, ACSL4 and FTH1 are not affected by ellipticine treatment (Fig. 7F), however, transferrin receptor (TFRC, a cell surface receptor essential for cellular iron uptake) is dose dependently down-regulated upon ellipticine treatment either in the absence or presence of RSL3 (Fig. 7E, G). We then measured the mRNA level of *TFRC* by qRT-PCR and found that ellipticine treatment reduces *TFRC* mRNA in either unstimulated or RSL3-stimulated cells (Fig. 7H). On the contrary, the mRNA level or protein level of *FTH1* (heavy chain of ferritin, which is the major intracellular iron storage protein) is unaffected by ellipticine treatment (Fig. 7E, H), indicating ellipticine does not affect iron metabolism globally. We then measured intracellular iron content and as expected, down-regulation of TFRC reduces cell iron content in ellipticine-treated cells (Fig. 7I). We also investigated whether a similar mechanism operates in zebrafish. Zebrafish has two transferrin receptor gene homologs (*tfr1a* and *tfr1b*) and we found ellipticine treatment reduces mRNA levels of both (Fig. 7J). Consistent with this, the protein level of transferrin receptors in total embryonic lysate is also reduced after ellipticine treatment (Fig. 7K). Together, these results indicate that ellipticine protects ferroptosis by downregulating *TFRC* expression and reducing cellular iron content in both HT1080 cells and zebrafish embryos.

Discussion

Zebrafish lateral line provides an accessible model to study hair cell development/ regeneration, or screen compounds for either ototoxic or otoprotective activities. Hair cell damages can be induced by a variety of ototoxic reagents including copper, cisplatin, or AGs while their underlying mechanisms are not fully understood. CuSO_4 has been reported to induce oxidative stress and necrotic hair cell death and it can be blocked by antioxidants [45], which is consistent with our finding here that Necrostatin-1 or NAC blocks CuSO_4 induced hair cell damages (Fig. 1F). Surprisingly, we found here that ferroptosis appears dispensable for CuSO_4 induced hair cell death, indicating that oxidative stress in hair cells does not necessarily lead to ferroptosis.

Cisplatin is a widely used chemotherapeutic reagent and ototoxicity is a major side effect in patients. Cisplatin-induced hair cell damages have been well documented in zebrafish. In a recent study, it is reported that the ferroptosis inhibitor Fer-1 protects cisplatin-induced ototoxicity in zebrafish hair cells [46] which

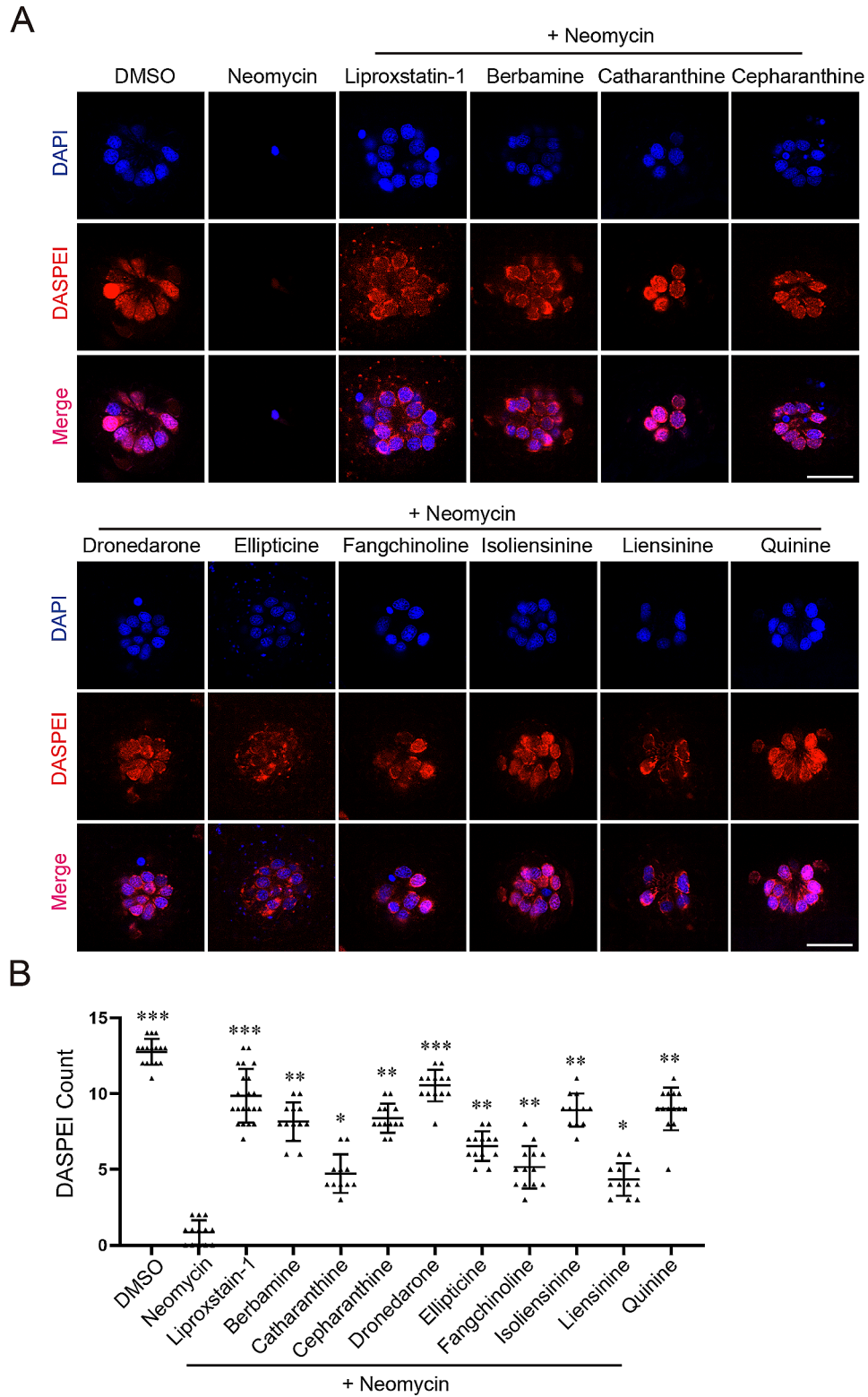


Fig. 4 Otoprotection screening against neomycin-induced hair cell damage in zebrafish lateral line. **A** Representative otoprotection results of the nine positive hit compounds identified from our screen. Liproxstatin-1 is a positive control. Scale bar: 20 μ m. **(B)** Quantitative results for **(A)**. Three biological repeats were performed and at least 10 larvae were analyzed for each treatment. *p*-value is determined by ordinary one-way ANOVA with Dunnett's multiple comparisons test. *, *p* < 0.05; **, *p* < 0.01; ***, *p* < 0.001

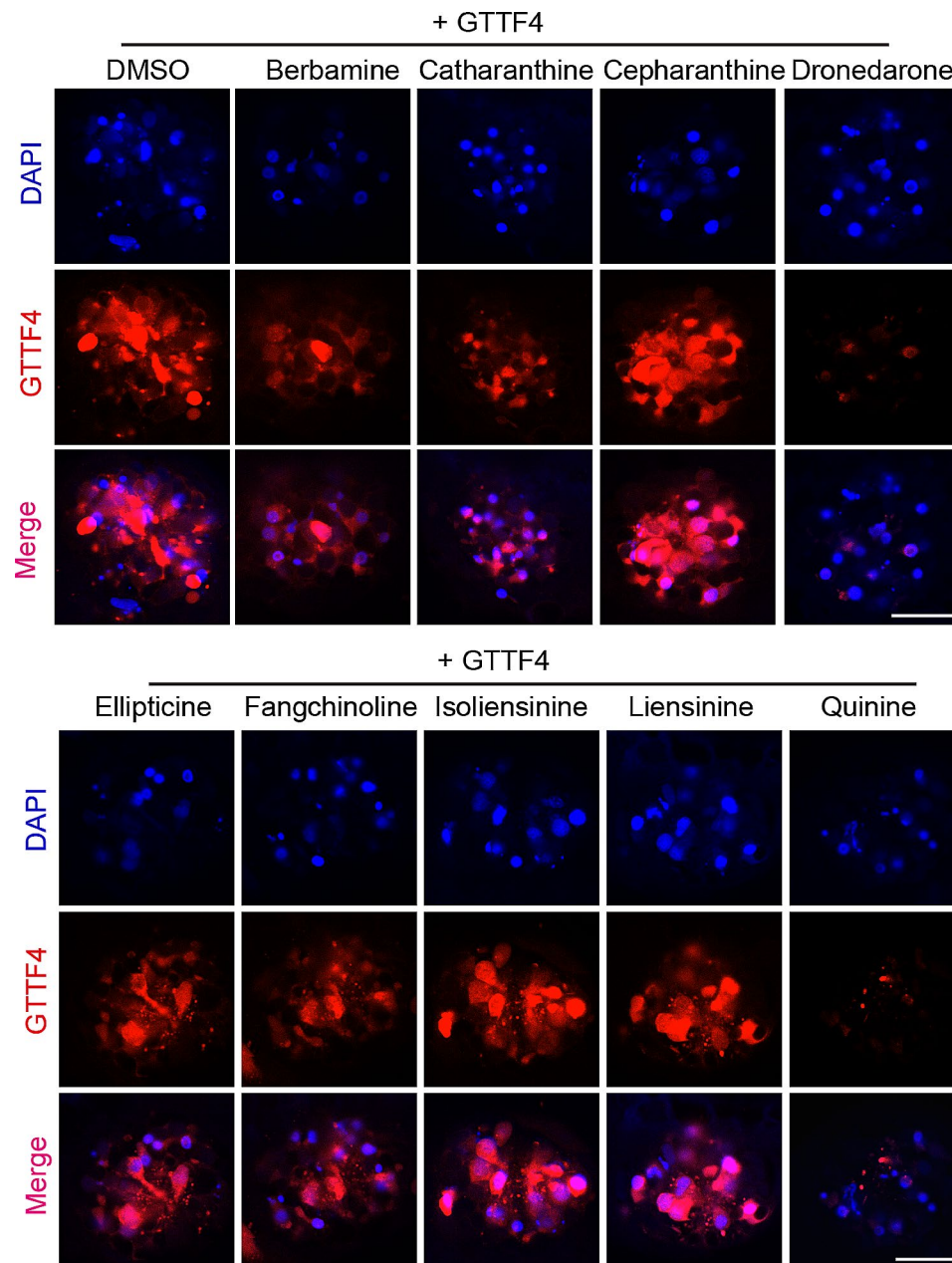


Fig. 5 Dronedarone and quinine block the uptake of GTTF4. GTTF4 loading assay were performed to evaluate the ability of a testing compound to block the uptake of GTTF4 in hair cells. Assays were repeated twice, and representative images are shown here. Scale bar: 20 μm

appears contradictory to our result that the ferroptosis inhibitor Liproxstatin-1 fails to protect cisplatin-induced hair cell death (Fig. 1E). Although both Fer-1 and Liproxstatin-1 show excellent ferroptosis inhibiting activity in cell cultures, Fer-1 is generally reported to be less effective and more toxic in vivo as ferroptosis inhibitor. In our hand, Fer-1 at 10, 20, or 40 μM all fails to block neomycin-induced hair cell death (data not shown) while Liproxstatin-1 at 10 μM is sufficient to protect neomycin ototoxicity (Fig. 1A). Thus, the inability of Liproxstatin-1 to block cisplatin-induced hair cell death cannot be

attributed to Liproxstatin-1 as a poor ferroptosis inhibitor in vivo, instead, it is more likely that ferroptosis does not contribute significantly to cisplatin-induced hair cell death under our assay condition. We notice that different cisplatin treatment protocols are used in these two studies (200 μM for 2 h vs. 40 μM for 24 h) which may lead to the activation of different intracellular death pathways and the observed inconsistency.

We revealed that ferroptosis is involved in hair cell damages induced by all AGs tested (neomycin, streptomycin, gentamycin, and amikacin) while apoptosis and

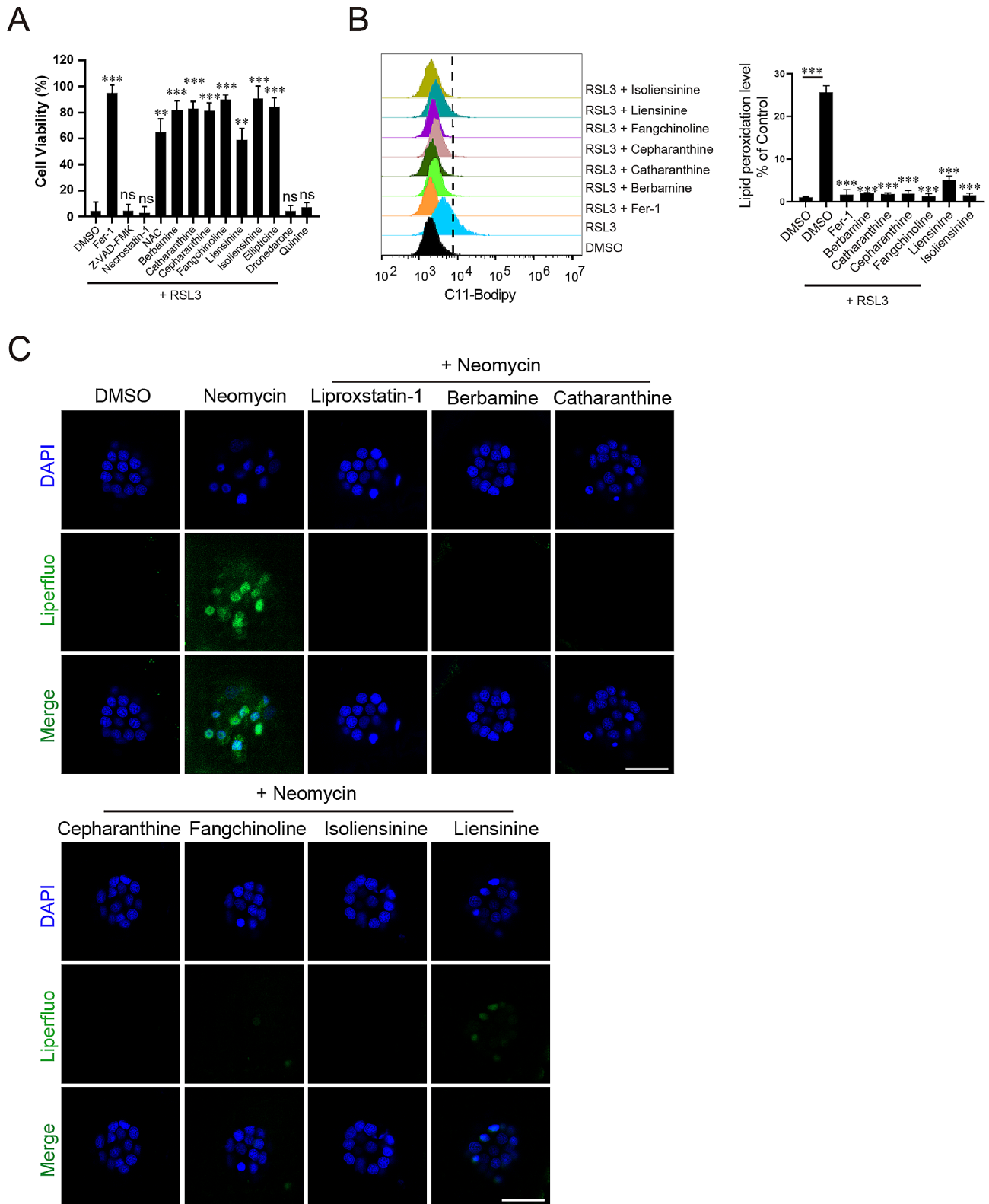


Fig. 6 Multiple hit compounds inhibit lipid ROS accumulation and ferroptosis. **A** All hit compounds other than dronedarone and quinine are able to inhibit RSL3-induced ferroptosis in HT1080 cells. Data represent mean \pm s.d. from three biological repeats and p -value is determined by ordinary one-way ANOVA with Dunnett’s multiple comparisons test. ns, no significance; **, $p < 0.01$; ***, $p < 0.001$. **B** FACS analysis of RSL3-induced lipid ROS in cells pre-treated with a hit compound. Data represent mean \pm s.d. from three biological repeats and p -value is determined by ordinary one-way ANOVA with Dunnett’s multiple comparisons test. ***, $p < 0.001$. **C** Hit compounds inhibit neomycin-induced lipid ROS accumulation in hair cells. Assays were performed and analyzed as described in Fig. 2B. Scale bar: 20 μ m

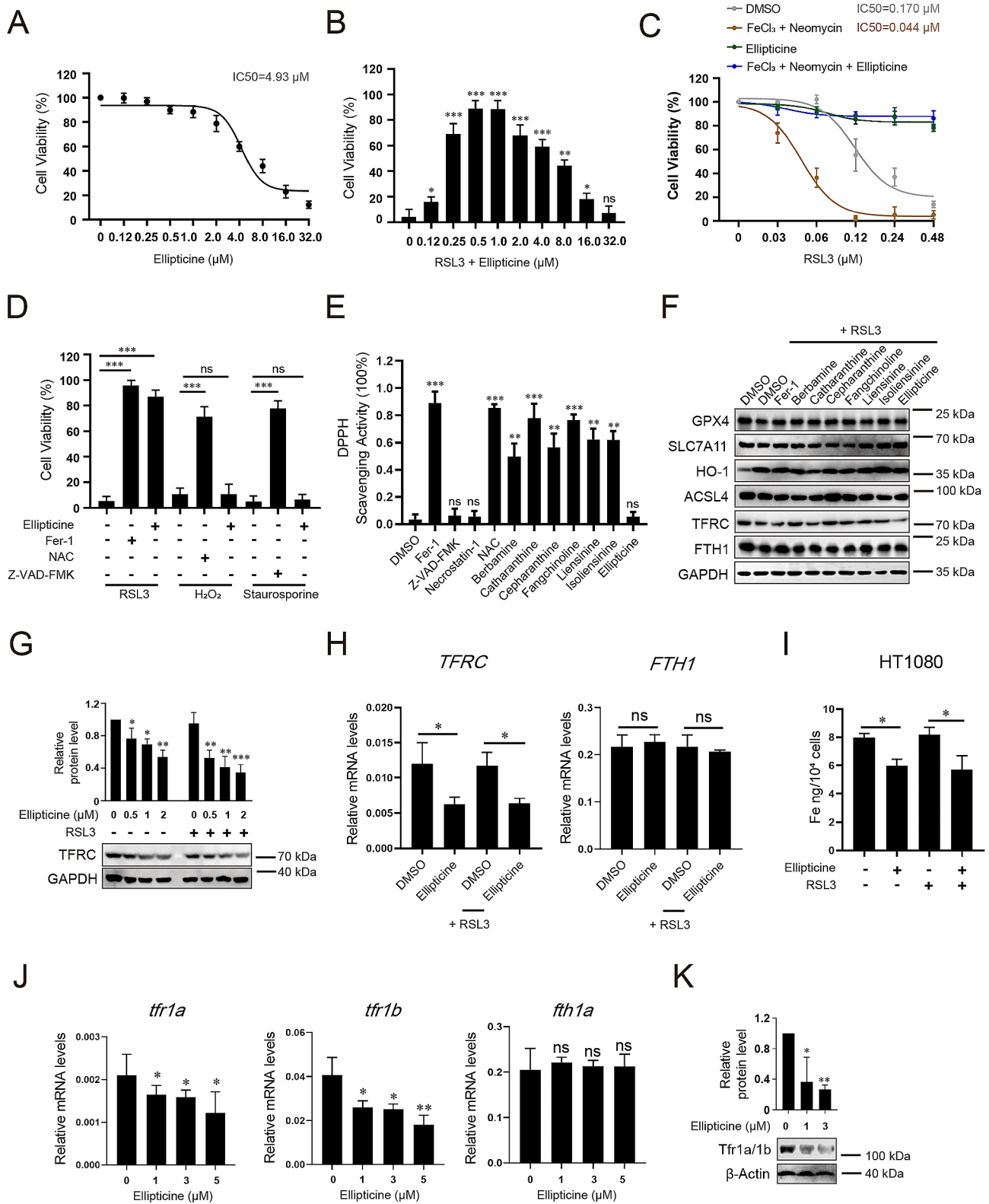


Fig. 7 (See legend on next page.)

(See figure on previous page.)

Fig. 7 Ellipticine inhibits ferroptosis by downregulation of TFRC and iron homeostasis. **A** Ellipticine toxicity assay in HT1080 cells. Data represent mean \pm s.d. from three biological repeats. **B** Protection of RSL3-induced cell death by the indicated concentrations of ellipticine. The best protection is achieved at 0.5 μ M. Data represent mean \pm s.d. from three repeats and *p*-value is determined by ordinary one-way ANOVA with Dunnett's multiple comparisons test. ns, no significance; *, *p* < 0.05; **, *p* < 0.01; ***, *p* < 0.001. **C** Ellipticine (0.5 μ M) protects neomycin/ Fe³⁺ stimulated ferroptosis sensitivity to RSL3. Assays were performed as described in Fig. 3A and data represent mean \pm s.d. from three biological repeats. **D** Ellipticine protects RSL3-induced (2 μ M) ferroptosis, but not hydrogen peroxide-induced (100 μ M) necroptosis or staurosporine-induced (2 μ M) apoptosis in HT1080 cells. Data represent mean \pm s.d. from three independent repeats and *p*-value is determined by ordinary one-way ANOVA with Tukey's multiple comparisons test. ns, no significance; ***, *p* < 0.001. **E** In vitro DPPH assay for ROS scavenging activity. Data represent mean \pm s.d. from three repeats and *p*-value is determined by student's *t*-test. ns, no significance; *, *p* < 0.05; **, *p* < 0.01; ***, *p* < 0.001. **F** Western blot for the indicated ferroptosis related proteins. The concentration used is 0.5 μ M (for ellipticine) or 5 μ M (for all other ferroptosis inhibiting compounds). GAPDH is the loading control. Assays were repeated twice, and representative blots are presented. **G** Ellipticine dose-dependently downregulates TFRC in either absence or presence of RSL3 in HT1080 cells. Representative western blots and quantitative results are presented. Data represent mean \pm s.d. of 4 blots and *p*-value is determined by ordinary one-way ANOVA with Dunnett's multiple comparisons test. *, *p* < 0.05; **, *p* < 0.01; ***, *p* < 0.001. **H** qRT-PCR analysis for *TFRC* and *FTH1* gene expression in HT1080 cells. β -actin is the internal control. Data represent mean \pm s.d. of three independent repeats and *p*-value is determined by student's *t*-test. ns, no significance; *, *p* < 0.05. **I** Cell iron content assay in HT1080 cells. Data represent mean \pm s.d. of three independent assays and *p*-value is determined by student's *t*-test. *, *p* < 0.05. **J** qRT-PCR analysis for zebrafish *tfr1a*, *tfr1b* and *fth1a* gene expression. β -actin is the internal control. Data represent mean \pm s.d. of three independent repeats and *p*-value is determined by ordinary one-way ANOVA with Dunnett's multiple comparisons test. ns, no significance; *, *p* < 0.05; **, *p* < 0.01. **K** Western blot for transferrin receptor expression in zebrafish total embryonic lysate. β -Actin is the loading control. A representative blot and quantitative results are presented. Data represent mean \pm s.d. of 3 blots and *p*-value is determined by ordinary one-way ANOVA with Dunnett's multiple comparisons test. *, *p* < 0.05; **, *p* < 0.01

necroptosis is activated by gentamicin and amikacin but not neomycin or streptomycin in these assays, indicating the activation of distinct intracellular death pathways by these AGs. Indeed, differences between neomycin- and gentamicin-induced hair cell deaths in zebrafish larvae have been reported in several previous studies. For example, neomycin-induced acute hair cell death is fully protected by pretreatment with the compound PROTO1 while gentamicin appears to induce hair cell death in biphasic manner: an acute phase that can be protected by PROTO1 and a chronic phase that cannot be protected by PROTO1 [47]. On the other hand, d-methionine treatment or overexpression of Bcl2 is able to block gentamicin but not neomycin induced ototoxicity [48, 49]. It will be interesting to test whether ferroptosis is responsible for these observed differences.

Inhibition the uptake of AGs is an effective way to protect AG-induced ototoxicity in zebrafish as well as other models. Small Compound screening in zebrafish have identified many otoprotectants that function to block the uptake of AGs. Our discovery that ferroptosis is the dominant cell death in neomycin-induced hair cell damage in zebrafish indicates that inhibition of ferroptosis could be another effective way to ameliorate neomycin-induced ototoxicity. To test this hypothesis, we performed a compound screening of alkaloid natural compound library which is known to be rich in antioxidants. We identified nine otoprotective compounds from this screen and two of them function to block neomycin uptake and seven of them inhibit ferroptosis, supporting an otoprotective function upon ferroptosis inhibition. Among the seven ferroptosis inhibiting compounds, berbamine, cepharanthine, fangchinoline, liensinine and isoliensinine are BBIQ compounds that were recently identified as ferroptosis inhibitors in our cell-based screen [44]. Catharanthine does not contain the chemical backbone of

BBIQ compounds, but it also has ROS scavenging activity (Fig. 7D) and shows ferroptosis inhibiting activity in cell-based assay (Fig. 6A). These data indicate that a compound's ferroptosis inhibiting activity in zebrafish hair cells largely predicts its activity in cell-based assay. Meanwhile, 15 out of the top 20 hits from our cell-based screen [44] are not otoprotective in vivo in neomycin-induced hair cell death assay, indicating ferroptosis inhibiting activity in cell-based assay does not guarantee otoprotective function in vivo, possibly due to factors such as compound stability, absorption, distribution, metabolism, toxicity, etc. Thus, positive hits from cell-based screen should be further validated in vivo in models such as zebrafish or mouse for their potential as candidate compounds for further drug development.

We noticed one compound, ellipticine, is not a top positive hit in our previous cell-based screen but protects neomycin-induced hair cell death in vivo. We further analyzed this compound and found that at the dose used in the previous screen (5 μ M) it is toxic to HT1080 cells, which prevents it be identified as a positive hit in the previous screen (Fig. 7B). We now show that ellipticine at sub-micromolar level is sufficient to inhibit ferroptosis in HT1080 cells via a unique mechanism: instead of scavenging lipid ROS, it downregulates intracellular iron content by inhibiting TFRC expression thus reduces the iron-dependent generation of lipid ROS. Downregulation of transferrin receptor by ellipticine is also observed in zebrafish embryos. Thus, it will be interesting to test whether ellipticine, by downregulating TFRC and cell iron content, has beneficial effects in the treatment of other iron-overload related disorders such as iron storage diseases.

In conclusion, our study reveals that neomycin stimulates ferroptosis in zebrafish lateral line hair cells as well as in in vitro cultured cell lines through mitochondrial

ROS pathway. Ferroptosis inhibition by stimulating the mitochondrial anti-ferroptotic DHODH/CoQ pathway, reducing intracellular iron content and lipid ROS generation, or promoting lipid ROS scavenging all show otoprotective activities. These results support the idea that, in addition to blocking the uptake of AGs, targeting intracellular death pathway can also be utilized to ameliorate AG-induced ototoxicity.

Materials and methods

Zebrafish ototoxicity assay

Zebrafish were maintained according to standard protocols (zfin.org) and AB strain wildtype zebrafish were used for all experiments. Animal experimental protocols were approved by the Institutional Animal Care and Use Committee at Guangzhou Institutes of Biomedicine and Health.

For otoprotection assay, zebrafish larvae at 5 *dpf* were cultured in 24-well plate (5–8 larvae per well in 1 ml E3 media (5 mM NaCl, 0.17 mM KCl, 0.33 mM CaCl₂ and 0.33 mM MgSO₄, pH 7.2)), then pretreated with Liproxstatin-1 (Selleck, S7699, 10 μM), Z-VAD-FMK (Selleck, S7023, 50 μM), Necrostatin-1 (Selleck, S8037, 50 μM) or NAC (Selleck, S1623, 5 mM) for 2 h, then treated with neomycin (Selleck, S2568, 125 μM), streptomycin (Selleck, S2572, 125 μM), gentamicin (Selleck, S4030, 125 μM), amikacin (Selleck, S3122, 125 μM), cisplatin (Selleck, S1166, 200 μM), or CuSO₄ (Macklin, C805233, 200 μM) for 2 h at 28°C. An alkaloid natural product library from TargetMol (TargetMol, Shanghai, China, L6110, 10 μM) were used to screen for compounds that can protect neomycin-induced hair cell death in zebrafish larvae. After treatment, larvae were washed with E3 media for 3 times, then stained with DASPEI (AAT Bioquest, 22225, 1 μM) and DAPI (Beyotime, C1005, 0.2 μg/mL) for 15 min at 28°C. Larvae were then washed with E3 media, embedded in 5% low-melting agarose then imaged using the Zeiss LSM800 confocal microscope. Assays were repeated two to three times and at least ten larvae were analyzed for each treatment.

ROS staining in larvae

For total ROS staining, larvae were treated with the indicated compounds as described above, washed with E3 media, then incubated in E3 containing DCFH-DA (Beyotime, S0033S, 10 μM) and DAPI (0.2 μg/mL) for 10 min in dark. Larvae were washed with E3, stimulated with 125 μM neomycin for 15 min, washed again with E3, then embedded in 5% low-melting agarose and ready for imaging using the Zeiss LSM800 confocal microscope. For lipid ROS staining, larvae were first incubated in Liperfluo (Dojindo, L248, 1 μM) and DAPI (0.2 μg/mL) for 20 min in dark. Larvae were then washed, then

stimulated with neomycin (125 μM, 5 min), then imaged as described above.

GTTF4 loading assay

Fluorescent labeling of gentamicin was performed by mixing Tide Fluor™ 4 (TF4, AAT Bioquest, 2289, 10 mg/mL in DMSO) with gentamicin (Topsience, T1362, 100 mM) (1:5 v/v) for 6–12 h at RT in dark which generates gentamicin-TF4 conjugate (GTTF4, 83 mM final concentration). Larvae were pretreated with the indicated testing compound (10 μM for 2 h), washed with E3, then incubated with GTTF4 (final concentration of 125 μM) and DAPI (0.2 μg/mL) for 15 min at 28°C. After incubation, larvae were washed with E3, fixed in 4% PFA (Beyotime, P0099) for 30 min at 4°C. Samples were then embedded in 5% low-melting agarose and imaged using the Zeiss LSM800 confocal microscope.

DPPH assay

The free radical scavenging capacity of a testing compound was assayed using the DPPH Assay Kit (Solarbio, BC4755). Briefly, NAC was diluted in the provided solution to the final concentration of 5 mM and all other testing compounds were diluted to 100 μM. An aliquot of testing compound solution (5 μL) was mixed thoroughly with 195 μL of DPPH working solution in 96-well plate and incubated in dark for 30 min at RT. After reaction, the absorbance (A) of the reaction mixture was assayed at the wavelength of 515 nm using an automatic microplate reader (Thermo, Epoch 2). The DPPH scavenging rate is calculated as: DPPH Scavenging Activity = $[(A \text{ blank} - (A \text{ sample} - A \text{ control})) / A \text{ blank}] \times 100\%$.

Cell viability assay

HT1080 cells were maintained in DMEM High Glucose cell culture medium (Gibco, 11995-065) supplemented with 10% fetal bovine serum (Gibco, 25,200,072) and 1% Penicillin-Streptomycin Solution (Solarbio, P1400) at 37°C with 5% CO₂. For rescuing assay, cells were cultured in 96-well plate (1 × 10⁴ cells per well) for 24 h, then stimulated with RSL3 (Selleck, S8155, 2 μM) together with a testing rescuing compound (Liproxstatin-1, 10 μM; Z-VAD-FMK, 50 μM; Necrostatin-1, 50 μM; NAC, 5 mM; other testing compound, all at 10 μM) for 24 h at 37°C. After the incubation, cell viability was assayed with the Cell Counting Kit-8 (CCK-8) (MCE, HY-K0301) according to the manufacturer's protocol. Assays were performed in triplicates and repeated three times.

Flow cytometry analysis of ROS

HT1080 cells were seeded on 12-well plates at the density of 1 × 10⁵ cells per well overnight then treated with the indicated compounds for 24 h. For detection of total ROS, cells were washed with serum-free DMEM then

incubated in DCFH-DA probe (Beyotime, Shanghai, China, S0033S, 10 μ M in serum-free medium) for 30 min at 37°C in dark. For detection of lipid ROS, treated cells were washed then incubated in BODIPY™ 581/591 C11 lipid ROS probe (Thermo, D3861, 2 μ M in serum-free media) for 1 h in dark at 37°C. For detection of mitochondrial ROS, cells were stained in MitoSOX™ Red (Thermo, M36008, 5 μ M in serum-free media) for 1 h in dark at 37°C. After dye incubation, cells were washed 3 times with serum-free medium, trypsinized with 200 μ L 0.25% Trypsin-EDTA (Gibico, 25,200,056). Trypsinization was terminated by 5% FBS/PBS and cells were collected by centrifugation at 1300 rpm for 3 min. Cells were resuspended in sterile 5% FBS/PBS, filtrated (70- μ m net), then analyzed using the BD Accuri C6 Plus Flow Cytometer (BD). Data were analyzed with the BD FlowJo V10 software.

Western blot

HT1080 cells were cultured in 24-well plates (1 \times 10⁵ cells per well) overnight then treated with the indicated compounds for 24 h as described above. After compound treatment, cells were lysed in 100 μ L of lysis buffer (a 4:1:0.01 mixture of Cell Lysis Buffer (Beyotime, P0013), 5 \times Loading Buffer (Beyotime, P0015L) and PMSF (Beyotime, ST506)) on ice for 5 min. For western blot analysis of zebrafish sample, embryos (1 *dpf*) were treated with ellipticine for 24 h then lysed in 150 μ L of lysis buffer on ice for 10 min. The mixture was then transferred to an EP tube and incubated in boiling water for 5 min. Samples were then centrifuged at 5,000 rpm for 1 min and supernatants were separated by 12% SDS-PAGE. After transferred to PVDF membranes (EMD Millipore, MA, IPVH00010), samples were blocked in solution (5% skim milk in TBST) for 1 h, washed with TBST for 3 times, then incubated with a primary antibody diluted in Quick-Block™ Primary Antibody Dilution Buffer for Western Blot (Beyotime, P0256) overnight at 4 °C. Blots were then washed with TBST and incubated with a HRP-conjugated secondary antibody (Goat Anti-Mouse IgG (H+L), Proteitech, Wuhan, China, SA00001-1, 1: 5000; or Goat Anti-Rabbit IgG (H+L), Proteitech, SA00001-2, 1: 5000) for 2 h at RT. Blots were then washed with TBST extensively, detected with the Immobilon Western Chemiluminescent HRP Substrate (EMD Millipore, WBKLS0100) and imaged using the GelView 6000 plus imaging system (BTL). Primary antibodies used for cell-based assay (HT1080) are: anti-GPX4 (1:1000, Abcam, Cambridge, UK, ab125066), anti-SLC7A11 (1:1000, Proteitech, 26864-1), anti-ACSL4 (1:1000, Abcam, ab205199), anti-FTH1 (1:1000, Abcam, ab75973), anti-TFRC (1:1000, Abcam, ab84036), anti-GAPDH (1:1000, Proteitech, HRP-60,004). Antibodies for zebrafish embryonic lysate

are anti-Tfr1a/b (1:2000, Proteitech, 66180-1-1g) and anti- β -Actin (1:1000, Proteitech, 66009-1-1g).

RNA extraction and qRT-PCR

Cells were cultured on 12-well plates and treated with the indicated compounds for 24 h. Zebrafish embryo (1 *dpf*) were treated with the indicated doses of ellipticine for 24 h. Total RNA was prepared with the Fast-Pure Cell/Tissue Total RNA Isolation Kit V2 (Vazyme, RC112-01) according to manufacturer's protocol. cDNA was synthesized using the HiScript Q RT SuperMix for qPCR Kit (Vazyme, R122-01) and PCR reaction was performed using the ChamQ SYBR qPCR Master Mix (Vazyme, Q331-02) on the CFX96 Touch Real-Time PCR Detection System (BioRad, CA). qPCR primers for human genes are: TFRC-F: ATCGGTTGGTGCCACT GAATGG; TFRC-R: ACAACAGTGGGCTGGCAGA AAC; β -Actin-F: CACCATGGCAATGAGCGGTTC; β -Actin-R: AGGTCTTTGCGGATGTCCACGT. qPCR primers for zebrafish genes are: tfr1a-F: GGCAGGACT GGTCCTCTTC; tfr1a-R: CCTGATCTGGGACACGT AGC; tfr1b-F: GGACTCTGTCCTGGTCAGC; tfr1b-R: GTCATGAACGAGACGGAGGG; fth1a-F: GAACAAG AGAGGTGGACGCA; fth1a-R: CAGCCCATTGTCCC ACTCAT; β -Actin-F: GGTATCGTGCTGGACTCTGG; β -Actin-R: GTGTGGCAGAGCATAACCCT.

Cell iron content assay

Cell iron concentration was detected with the Cell Iron Content Assay Kit according to manufacturer's protocol (Solarbio, BC5315). Briefly, 2.5 \times 10⁶ cells were treated with the indicated compounds for 24 h, trypsinized with 500 μ L 0.25% Trypsin-EDTA then terminated by 5% FBS DMEM High Glucose cell culture medium. Cells were collected by centrifugation at 1300 rpm for 3 min. Cells were treated with 500 μ L extraction reagent and ultrasonicated for 1 min, centrifuged at 10,000 rpm for 10 min. An aliquot of supernatant (20 μ L) was mixed with iron detection reagent for 10 min at RT then absorbance measured at 510 nm. Cell iron content (ng/10,000 cell)=27.922 \times (A sample - A control) \div (A standard-sample - A control).

Statistical analyses

Statistical analyses were performed using the GraphPad Prism 8.0.2 software (GraphPad Software, CA). Data were collected from 3 independent biological repeats and expressed as means \pm s.d. Statistical significance was determined using student's t-test, ordinary one-way or two-way ANOVA, and *p*-value<0.05 were considered statistically significant.

Abbreviations

AGs	Aminoglycoside antibiotics
ROS	Reactive oxygen species

RTAs	Radical trapping agents
<i>dpf</i>	<i>Day post fertilization</i>
NAC	N-acetylcysteine
DASPEI	2-[4-(Dimethylamino)styryl]-1-ethylpyridinium iodide
DAPI	4',6-Diamidino-2-phenylindole
DCFH-DA	Dichlorodihydrofluorescein diacetate
DHO	Dihydroorotate
BBIQ	Bisbenzylisoquinoline
GTTF4	Gentamicin-TF4 conjugate
TFRC	Transferrin receptor
FTTH1	Heavy chain of ferritin

Supplementary Information

The online version contains supplementary material available at <https://doi.org/10.1186/s13578-024-01258-w>.

Supplementary Material 1

Supplementary Material 2

Acknowledgements

We would like to thank GIBH core facility and other members of our lab for technical support.

Author contributions

XS conceived the project. YF and YZ conducted the experiments and analyzed the data. DQ provided reagents and additional support. YF and XS wrote and revised the manuscript. All authors proved the final version of the manuscript.

Funding

This work is supported by Basic Research Project of Guangzhou Institutes of Biomedicine and Health, Chinese Academy of Sciences (GIBHRP23-02) and Science and Technology Planning Project of Guangdong Province (2020B1212060052).

Data availability

All data generated or analyzed during this study are included in this published article and its supplementary information files.

Declarations

Ethics approval and consent to participate
Not applicable.

Consent for publication
Not applicable.

Competing interests

The authors declare that they have no competing interests.

Received: 23 February 2024 / Accepted: 29 May 2024

Published online: 05 June 2024

References

- O'Sullivan ME, Perez A, Lin R, Sajjadi A, Ricci AJ, Cheng AG. Towards the Prevention of Aminoglycoside-related hearing loss. *Front Cell Neurosci*. 2017;11:325.
- Kros CJ, Steyger PS. Aminoglycoside- and Cisplatin-Induced Ototoxicity: mechanisms and otoprotective strategies. *Cold Spring Harbor Perspect Med*. 2019;9(11):1–18.
- Kim J, Hemachandran S, Cheng AG, Ricci AJ. Identifying targets to prevent aminoglycoside ototoxicity. *Mol Cell Neurosci*. 2022;120:103722.
- Fu X, Wan P, Li P, Wang J, Guo S, Zhang Y, An Y, Ye C, Liu Z, Gao J, et al. Mechanism and Prevention of Ototoxicity Induced by aminoglycosides. *Front Cell Neurosci*. 2021;15:692762.
- Steyger PS. Mechanisms of Aminoglycoside- and Cisplatin-Induced Ototoxicity. *Am J Audiol*. 2021;30(35):887–900.
- Tan WJT, Song L. Role of mitochondrial dysfunction and oxidative stress in sensorineural hearing loss. *Hear Res*. 2023;434:108783.
- Stockwell BR, Jiang X, Gu W. Emerging mechanisms and Disease Relevance of Ferroptosis. *Trends Cell Biol*. 2020;30(6):478–90.
- Zheng J, Conrad M. The metabolic underpinnings of Ferroptosis. *Cell Metabol*. 2020;32(6):920–37.
- Tang D, Chen X, Kang R, Kroemer G. Ferroptosis: molecular mechanisms and health implications. *Cell Res*. 2021;31(2):107–25.
- Dixon SJ, Lemberg KM, Lamprecht MR, Skouta R, Zaitsev EM, Gleason CE, Patel DN, Bauer AJ, Cantley AM, Yang WS, et al. Ferroptosis: an iron-dependent form of nonapoptotic cell death. *Cell*. 2012;149(5):1060–72.
- Gan B. Mitochondrial regulation of ferroptosis. *J Cell Biol*. 2021;220(9).
- Stockwell BR, Jiang X. The Chemistry and Biology of Ferroptosis. *Cell Chem Biol*. 2020;27(4):365–75.
- Dehne N, Rauen U, de Groot H, Lautermann J. Involvement of the mitochondrial permeability transition in gentamicin ototoxicity. *Hear Res*. 2002;169(1–2):47–55.
- Song BB, Schacht J. Variable efficacy of radical scavengers and iron chelators to attenuate gentamicin ototoxicity in guinea pig in vivo. *Hear Res*. 1996;94(1–2):87–93.
- Conlon BJ, Perry BP, Smith DW. Attenuation of neomycin ototoxicity by iron chelation. *Laryngoscope*. 1998;108(2):284–7.
- Chang J, Choi J, Rah YC, Yoo MH, Oh KH, Im GJ, Lee SH, Kwon SY, Park HC, Chae SW, et al. Sodium Selenite acts as an otoprotectant against neomycin-Induced Hair cell damage in a zebrafish model. *PLoS ONE*. 2016;11(3):e0151557.
- Zheng Z, Tang D, Zhao L, Li W, Han J, Hu B, Nie G, He Y. Liproxstatin-1 Protects Hair Cell-Like HEI-OC1 Cells and Cochlear Hair Cells against Neomycin Ototoxicity. *Oxidative medicine and cellular longevity*. 2020;2020:1782659.
- Barrallo-Gimeno A, Llorens J. Hair cell toxicology: with the help of a little fish. *Front cell Dev Biology*. 2022;10:1085225.
- Harris JA, Cheng AG, Cunningham LL, MacDonald G, Raible DW, Rubel EW. Neomycin-induced hair cell death and rapid regeneration in the lateral line of zebrafish (*Danio rerio*). *J Association Res Otolaryngology: JARO*. 2003;4(2):219–34.
- Ton C, Parg C. The use of zebrafish for assessing ototoxic and otoprotective agents. *Hear Res*. 2005;208(1–2):79–88.
- Owens KN, Cunningham DE, MacDonald G, Rubel EW, Raible DW, Pujol R. Ultrastructural analysis of aminoglycoside-induced hair cell death in the zebrafish lateral line reveals an early mitochondrial response. *J Comp Neurol*. 2007;502(4):522–43.
- Esterberg R, Linbo T, Pickett SB, Wu P, Ou HC, Rubel EW, Raible DW. Mitochondrial calcium uptake underlies ROS generation during aminoglycoside-induced hair cell death. *J Clin Investig*. 2016;126(9):3556–66.
- Chang J, Im GJ, Chae SW, Lee SH, Kwon SY, Jung HH, Chung AY, Park HC, Choi J. Protective role of Trimetazidine against neomycin-induced hair cell damage in zebrafish. *Clin Exp Otorhinolaryngol*. 2013;6(4):219–25.
- Choi J, Chang J, Jun HJ, Im GJ, Chae SW, Lee SH, Kwon SY, Jung HH, Chung AY, Park HC. Protective role of edaravone against neomycin-induced ototoxicity in zebrafish. *J Appl Toxicology: JAT*. 2014;34(5):554–61.
- Song JJ, Chang J, Choi J, Im GJ, Chae SW, Lee SH, Kwon SY, Jung HH, Chung AY, Park HC, et al. Protective role of NecroX-5 against neomycin-induced hair cell damage in zebrafish. *Arch Toxicol*. 2014;88(2):435–41.
- Rah YC, Choi J, Yoo MH, Yum G, Park S, Oh KH, Lee SH, Kwon SY, Cho SH, Kim S, et al. Ecabet sodium alleviates neomycin-induced hair cell damage. *Free Radic Biol Med*. 2015;89:1176–83.
- Hirose Y, Sugahara K, Kanagawa E, Takemoto Y, Hashimoto M, Yamashita H. Quercetin protects against hair cell loss in the zebrafish lateral line and guinea pig cochlea. *Hear Res*. 2016;342:80–5.
- Kruger M, Boney R, Ordoobadi AJ, Sommers TF, Trapani JG, Coffin AB. Natural bisbenzoquinoline derivatives protect zebrafish lateral line sensory hair cells from Aminoglycoside Toxicity. *Front Cell Neurosci*. 2016;10:83.
- Hudson AM, Lockard GM, Namjoshi OA, Wilson JW, Kindt KS, Blough BE, Coffin AB. Berbammine analogs exhibit Differential Protective effects from Aminoglycoside-Induced Hair Cell Death. *Front Cell Neurosci*. 2020;14:234.
- Kirkwood NK, O'Reilly M, Derudas M, Kenyon EJ, Huckvale R, van Netten SM, Ward SE, Richardson GP, Kros CJ. d-Tubocurarine and Berbammine: Alkaloids that are permeant blockers of the Hair Cell's Mechano-Electrical Transducer Channel and protect from Aminoglycoside Toxicity. *Front Cell Neurosci*. 2017;11:262.

31. Kitcher SR, Kirkwood NK, Camci ED, Wu P, Gibson RM, Redila VA, Simon JA, Rubel EW, Raible DW, Richardson GP et al. ORC-13661 protects sensory hair cells from aminoglycoside and cisplatin ototoxicity. *JCI Insight* 2019, 4(15).
32. Owens KN, Santos F, Roberts B, Linbo T, Coffin AB, Knisely AJ, Simon JA, Rubel EW, Raible DW. Identification of genetic and chemical modulators of zebrafish mechanosensory hair cell death. *PLoS Genet.* 2008;4(2):e1000020.
33. Ou HC, Cunningham LL, Francis SP, Brandon CS, Simon JA, Raible DW, Rubel EW. Identification of FDA-approved drugs and bioactives that protect hair cells in the zebrafish (*Danio rerio*) lateral line and mouse (*Mus musculus*) utricle. *J Association Res Otolaryngology: JARO.* 2009;10(2):191–203.
34. Vlasits AL, Simon JA, Raible DW, Rubel EW, Owens KN. Screen of FDA-approved drug library reveals compounds that protect hair cells from aminoglycosides and cisplatin. *Hear Res.* 2012;294(1–2):153–65.
35. Kenyon EJ, Kirkwood NK, Kitcher SR, O'Reilly M, Derudas M, Cantillon DM, Goodyear RJ, Secker A, Baxendale S, Bull JC et al. Identification of ion-channel modulators that protect against aminoglycoside-induced hair cell death. *JCI insight* : 2017, 2(24).
36. Kenyon EJ, Kirkwood NK, Kitcher SR, Goodyear RJ, Derudas M, Cantillon DM, de la Baxendale S, Mahieu VN, Osgood RT et al. Identification of a series of hair-cell MET channel blockers that protect against aminoglycoside-induced ototoxicity. *JCI insight* : 2021, 6(7).
37. Zallocchi M, Hati S, Xu Z, Hausman W, Liu H, He DZ, Zuo J. Characterization of quinoxaline derivatives for protection against iatrogenically induced hearing loss. *JCI Insight* 2021, 6(5).
38. Friedmann Angeli JP, Schneider M, Proneth B, Tyurina YY, Tyurin VA, Hammond VJ, Herbach N, Aichler M, Walch A, Eggenhofer E, et al. Inactivation of the ferroptosis regulator Gpx4 triggers acute renal failure in mice. *Nat Cell Biol.* 2014;16(12):1180–91.
39. Gregory-Evans CY, Moosajee M, Shan X, Gregory-Evans K. Gene-specific differential response to anti-apoptotic therapies in zebrafish models of ocular coloboma. *Mol Vis.* 2011;17:1473–84.
40. Viringipurampeer IA, Ferreira T, DeMaria S, Yoon JJ, Shan X, Moosajee M, Gregory-Evans K, Ngai J, Gregory-Evans CY. Pax2 regulates a fadd-dependent molecular switch that drives tissue fusion during eye development. *Hum Mol Genet.* 2012;21(10):2357–69.
41. Hernandez PP, Moreno V, Olivari FA, Allende ML. Sub-lethal concentrations of waterborne copper are toxic to lateral line neuromasts in zebrafish (*Danio rerio*). *Hear Res.* 2006;213(1–2):1–10.
42. Lesniak W, Pecoraro VL, Schacht J. Ternary complexes of gentamicin with iron and lipid catalyze formation of reactive oxygen species. *Chem Res Toxicol.* 2005;18(2):357–64.
43. Mao C, Liu X, Zhang Y, Lei G, Yan Y, Lee H, Koppula P, Wu S, Zhuang L, Fang B, et al. DHODH-mediated ferroptosis defence is a targetable vulnerability in cancer. *Nature.* 2021;593(7860):586–90.
44. Fan Y, Zhang Y, Shi K, Cheng S, Pei D, Shu X. Identification of a group of bisbenzylisoquinoline (BBIQ) compounds as ferroptosis inhibitors. *Cell Death Dis.* 2022;13(11):1000.
45. Olivari FA, Hernandez PP, Allende ML. Acute copper exposure induces oxidative stress and cell death in lateral line hair cells of zebrafish larvae. *Brain Res.* 2008;1244:1–12.
46. Hu B, Liu Y, Chen X, Zhao J, Han J, Dong H, Zheng Q, Nie G. Ferrostatin-1 protects auditory hair cells from cisplatin-induced ototoxicity in vitro and in vivo. *Biochem Biophys Res Commun.* 2020;533(4):1442–8.
47. Owens KN, Coffin AB, Hong LS, Bennett KO, Rubel EW, Raible DW. Response of mechanosensory hair cells of the zebrafish lateral line to aminoglycosides reveals distinct cell death pathways. *Hear Res.* 2009;253(1–2):32–41.
48. Coffin AB, Rubel EW, Raible DW. Bax, Bcl2, and p53 differentially regulate neomycin- and gentamicin-induced hair cell death in the zebrafish lateral line. *J Association Res Otolaryngology: JARO.* 2013;14(5):645–59.
49. Coffin AB, Williamson KL, Mamiya A, Raible DW, Rubel EW. Profiling drug-induced cell death pathways in the zebrafish lateral line. *Apoptosis: Int J Program cell Death.* 2013;18(4):393–408.

Publisher's Note

Springer Nature remains neutral with regard to jurisdictional claims in published maps and institutional affiliations.